Eur. Phys. J. C 40, 515–517 (2005)
Digital Object Identifier (DOI) 10.1140/epjc/s2005-02167-3

THE EUROPEAN PHYSICAL JOURNAL C

Probing the perturbative NLO parton evolution in the small-x region

M. Glück, C. Pisano, E. Reya

Universität Dortmund, Institut für Physik, 44221 Dortmund, Germany

Received: 6 December 2004 / Revised version: 1 February 2005 /
Published online: 9 March 2005 –

Abstract. A dedicated test of the perturbative QCD NLO parton evolution in the very small-x region is performed. We find a good agreement with recent precision HERA data for $F_2^{\rm p}(x, Q^2)$, as well as with the present determination of the curvature of $F_2^{\rm p}$. Characteristically, perturbative QCD evolutions result in a positive curvature which increases as x decreases. Future precision measurements in the very small x-region, $x < 10^{-4}$, could provide a sensitive test of the range of validity of perturbative QCD.

Parton distributions $f(x, Q^2)$, $f = q, \bar{q}, g$, underlie the Q^2-evolution dictated by perturbative QCD at $Q^2 \gtrsim 1\,{\rm GeV}^2$. It was recently stated [1] that the NLO perturbative QCD Q^2-evolution disagrees with HERA data [2,3] on $F_2^{\rm p}(x, Q^2)$ in the small-x region, $x \lesssim 10^{-3}$. In view of the importance of this statement we perform here an independent study of this issue. In contrast to [1] we shall undertake this analysis in the standard framework where one sets up input distributions at some low Q_0^2, here taken to be $Q_0^2 = 1.5\,{\rm GeV}^2$, corresponding to the lowest Q^2 considered in [1], and adapting these distributions to the data considered. In the present case the data considered will be restricted to

$$1.5\,{\rm GeV}^2 \leq Q^2 \leq 12\,{\rm GeV}^2, \quad 3\times10^{-5} \lesssim x \lesssim 3\times10^{-3} \tag{1}$$

as in [1] and will be taken from the corresponding measured $F_2^{\rm p}(x, Q^2)$ of the H1 collaboration [2]. The choice of these data is motivated by their higher precision as compared to corresponding data of the ZEUS collaboration [3], in particular in the very small-x region.

We shall choose two sets of input distributions based on the GRV98 parton distributions [4]. In the first set we shall adopt u_v, d_v, $s = \bar{s}$ and $\Delta \equiv \bar{d} - \bar{u}$ from GRV98 and modify $\bar{u} + \bar{d}$ and the gluon distribution in the small-x region to obtain an optimal fit to the H1 data [2] in the aforementioned kinematical region. We shall refer to this fit as the "best fit". The second choice will be constrained to modify the GRV98 $\bar{u} + \bar{d}$ and g distributions in the small-x region as little as possible. We shall refer to this fit as GRV$_{\rm mod}$. It will turn out that both input distributions are compatible with the data to practically the same extent, i.e. yielding comparable χ^2/dof. In view of these observations we do not agree with the conclusions of [1], i.e. we do not confirm a disagreement between the NLO Q^2-evolution of $f(x, Q^2)$ and the measured [2,3] Q^2-dependence of $F_2^{\rm p}(x, Q^2)$.

The remaining flavor-singlet input distributions at $Q_0^2 = 1.5\,{\rm GeV}^2$ to be adapted to the recent small-x data are expressed as

$$\begin{aligned} &xg(x, Q_0^2) \\ &\quad = N_g x^{-a_g}\left(1 + A_g\sqrt{x} + 7.283x\right)(1-x)^{4.759}, \end{aligned} \tag{2}$$

$$\begin{aligned} &x(\bar{u} + \bar{d})(x, Q_0^2) \\ &\quad = N_s a^{-a_s}\left(1 + A_s\sqrt{x} - 4.046x\right)(1-x)^{4.225}, \end{aligned} \tag{3}$$

where the parameters relevant for the large-x region, $x > 10^{-3}$, which is of no relevance for the present small-x studies, are kept unchanged and are taken from, e.g. GRV98 [4]. The refitted relevant small-x parameters turn out to be

$$\begin{aligned} \text{"best fit"}: &\ N_g = 1.70\,, \quad a_g = 0.027\,, \quad A_g = -1.034, \\ &\ N_s = 0.171\,, \quad a_s = 0.177\,, \quad A_s = 2.613, \end{aligned} \tag{4}$$

$$\begin{aligned} {\rm GRV_{mod}}: &\ N_g = 1.443\,, \quad a_g = 0.125\,, \quad A_g = -2.656, \\ &\ N_s = 0.270\,, \quad a_s = 0.117\,, \quad A_s = 1.70, \end{aligned} \tag{5}$$

to be compared with the original GRV98 parameters [4]: $N_g = 1.443$, $a_g = 0.147$, $A_g = -2.656$ and $N_s = 0.273$, $a_s = 0.121$, $A_s = 1.80$. The resulting predictions are compared to the H1 data [2] in Fig. 1. These results are also consistent with the ZEUS data [3] with partly lower statistics. The corresponding χ^2/dof are 0.50 for the "best fit" (dof = 48) and 0.94 for GRV$_{\rm mod}$ (dof = 50), respectively. Our treatment of the heavy flavor contributions to F_2 differs from that in [1]. We evaluate these contributions in the fixed flavor $f = 3$ scheme of [4], together with the massive heavy quark (c, b) contributions, rather than in the $f = 4$ (massless) scheme utilized in [1]. We have checked, however, that our disagreement with [1] does *not* result from our $f = 3$ plus heavy quarks versus the $f = 4$ massless quark calculations in [1]: we have also performed a fit for $f = 4$

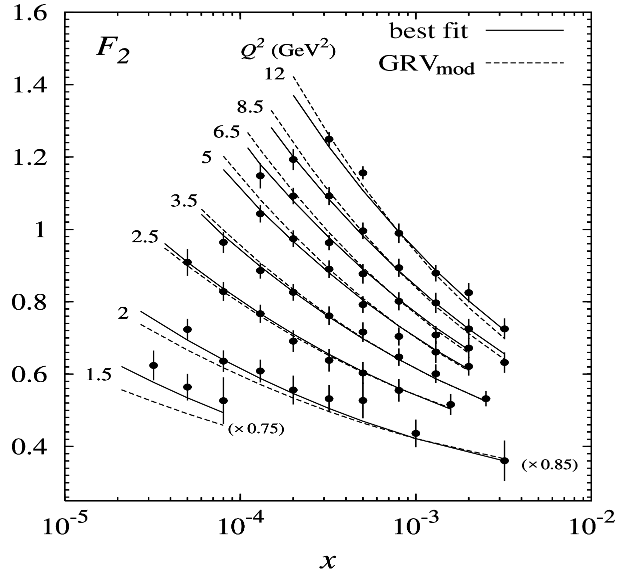

Fig. 1. Comparison of our "best fit" and $\mathrm{GRV_{mod}}$ results based on (4) and (5), respectively, with the H1 data [2]. To ease the graphical representation, the results and data for the lowest bins in $Q^2 = 1.5\,\mathrm{GeV}^2$ and $2\,\mathrm{GeV}^2$ have been multiplied by 0.75 and 0.85, respectively, as indicated

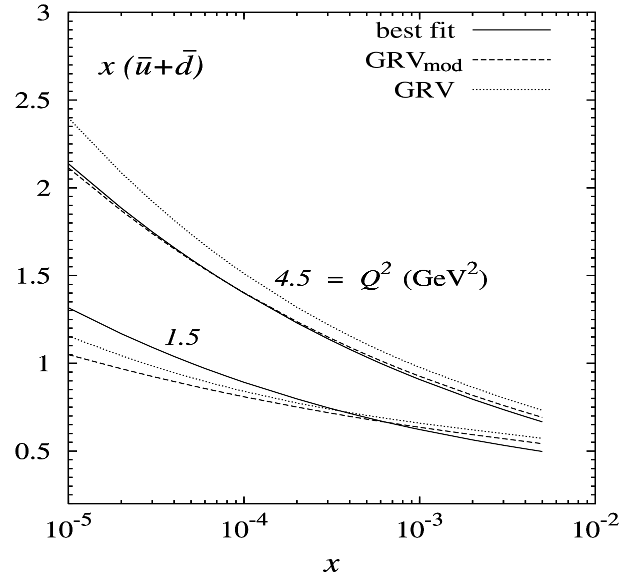

Fig. 3. The sea distribution $x(\bar{u}+\bar{d})$ at the input scale $Q_0^2 = 1.5\,\mathrm{GeV}^2$ in (3) with the "best fit" and $\mathrm{GRV_{mod}}$ parameters in (4) and (5), respectively, and at $Q^2 = 4.5\,\mathrm{GeV}^2$. For comparison, the original GRV98 results [4] are shown as well by the dotted curves

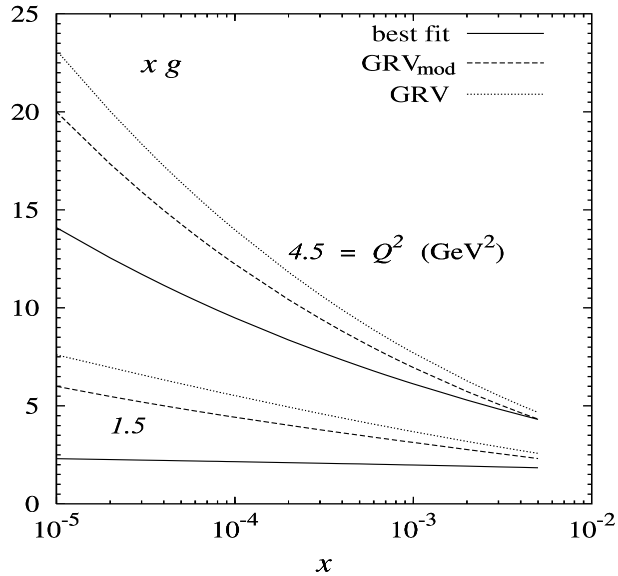

Fig. 2. The gluon distributions at the input scale $Q_0^2 = 1.5\,\mathrm{GeV}^2$ corresponding to (2) with the "best fit" and $\mathrm{GRV_{mod}}$ parameters in (4) and (5), respectively, and at $Q^2 = 4.5\,\mathrm{GeV}^2$. For comparison, the original GRV98 results [4] are shown as well by the dotted curves

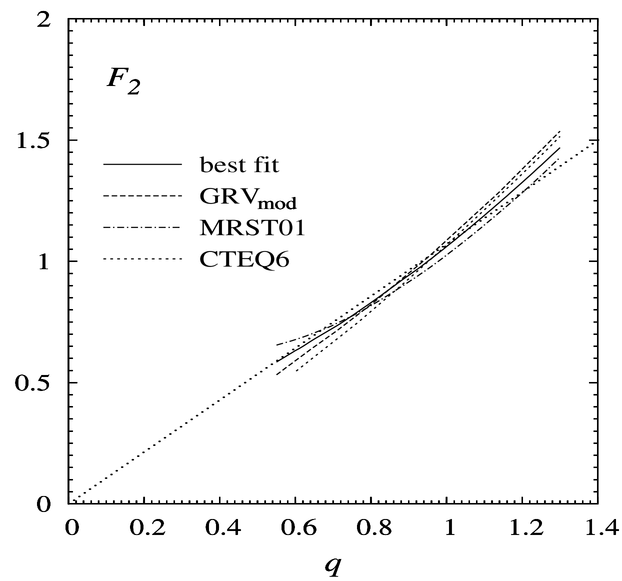

Fig. 4. Predictions for $F_2(x,Q^2)$ at $x = 10^{-4}$ plotted versus q defined in (6). Representative global fit results are taken from MRST01 [5] and CTEQ6M [6]. Most small-x measurements lie along the straight (dotted) line [1]

massless quarks and the results for F_2 and its curvature, to be discussed below, remain essentially unchanged.

In Figs. 2 and 3 we show our gluon and sea input distributions in (2) and (3), as well as their evolved shapes at $Q^2 = 4.5\,\mathrm{GeV}^2$ in the small-x region. It can be seen that both of our new small-x gluon distributions at $Q^2 = 4.5\,\mathrm{GeV}^2$ conform to the rising shape obtained in most available analyses published so far, in contrast to the valence-like shape obtained in [1] where the gluon density xg decreases as $x \to 0$. It is possible to conceive a valence-like gluon at some very low Q^2 scale, as in [4], but even in this extreme case the gluon ends up as non-valence-like at $Q^2 > 1\,\mathrm{GeV}^2$, in particular at $Q^2 = 4.5\,\mathrm{GeV}^2$, as physically expected.

Turning now to the curvature test of F_2 advocated and discussed in [1], we first present in Fig. 4 our results for $F_2(x,Q^2)$ at $x = 10^{-4}$, together with two representative expectations of global fits [5,6], as a function of [1]

$$q = \log_{10}\left(1 + \frac{Q^2}{0.5\,\mathrm{GeV}^2}\right). \qquad (6)$$

This variable has the advantage that most measurements lie along a straight line [1] as indicated by the dotted line at $x = 10^{-4}$ in Fig. 4. The MRST01 parametrization [5] results in a sizable curvature for F_2 in contrast to all other fits shown in Fig. 4. This large curvature, incompatible with the data presented in [1], is mainly caused by the valence-like input gluon distribution of MRST01 at $Q_0^2 = 1\,\mathrm{GeV}^2$ in the small-x region which becomes even negative for $x < 10^{-3}$ [5]. A similar result was obtained in [1] based on a particular gluon distribution $xg(x, Q^2)$ which decreases with decreasing x for $x \lesssim 10^{-3}$ even at $Q^2 = 4.5\,\mathrm{GeV}^2$ (cf. Fig. 7 in [1]). More explicitly the curvature can be directly extracted from

$$F_2(x, Q^2) = a_0(x) + a_1(x)q + a_2(x)q^2\,. \qquad (7)$$

The curvature $a_2(x) = \frac{1}{2}\,\partial_q^2 F_2(x, Q^2)$ is evaluated by fitting the predictions for $F_2(x, Q^2)$ at fixed values of x to a (kinematically) given interval of q. In Fig. 5a we present $a_2(x)$ which results from experimentally selected q-intervals [1]:

$$\begin{aligned} &0.7 \le q \le 1.4 \text{ for } 2\times10^{-4} < x < 10^{-2},\\ &0.7 \le q \le 1.2 \text{ for } 5\times10^{-5} < x \le 2\times10^{-4},\\ &0.6 \le q \le 0.8 \text{ for } x = 5\times10^{-5}\,. \end{aligned} \qquad (8)$$

Notice that the average value of q decreases with decreasing x due to the kinematically more restricted Q^2 range accessible experimentally. For comparison we also show in Fig. 5b the curvature $a_2(x)$ for an x-independent fixed q-interval

$$0.6 \le q \le 1.4 \qquad (1.5\,\mathrm{GeV}^2 \le Q^2 \le 12\,\mathrm{GeV}^2)\,. \qquad (9)$$

Apart from the rather large values of $a_2(x)$ specific for the MRST01 fit as discussed above (cf. Fig. 4), our “best fit” and $\mathrm{GRV_{mod}}$ results, based on the inputs in (4) and (5), respectively, do agree well with the experimental curvatures as calculated and presented in [1] using H1 data. It should be noted that perturbative NLO evolutions result in a *positive* curvature $a_2(x)$ which increases as x decreases. This feature is supported by the data shown in Fig. 5a; since the data point at $x < 10^{-4}$ is statistically insignificant, future precision measurements in this very small-x region should provide a sensitive test of the range of validity of perturbative QCD evolutions.

Furthermore, the H1 collaboration [2] has found a good agreement between the perturbative NLO evolution and the slope of $F_2(x, Q^2)$, i.e. the *first* derivative $\partial_{Q^2} F_2$.

To conclude, the perturbative NLO evolution of parton distributions in the small-x region is compatible with recent high-statistics measurements of the Q^2-dependence of $F_2^{\mathrm{p}}(x, Q^2)$ in that region. A characteristic feature of perturbative QCD evolutions is a *positive* curvature $a_2(x)$ which increases as x decreases (cf. Fig. 5). Although present data are indicative for such a behavior, they are statistically insignificant for $x < 10^{-4}$. Future precision measurements and the ensuing improvements of the determination of the curvature in the very small-x region should provide further information concerning the detailed shapes of the gluon and sea distributions and perhaps may even provide a sensitive test of the range of validity of perturbative QCD.

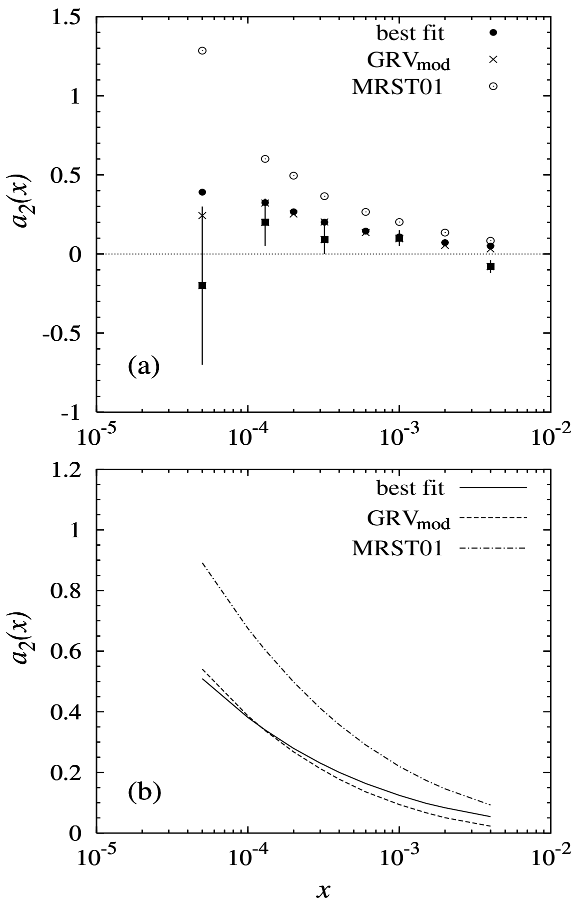

Fig. 5. The curvature $a_2(x)$ as defined in (7) for **a** the variable q-intervals in (8) and **b** the fixed q-interval in (9). Also shown are the corresponding MRST01 results [5]. The experimental curvatures (squares) shown in **a** are taken from [1]

Acknowledgements. This work has been supported in part by the Bundesministerium für Bildung und Forschung, Berlin/Bonn.

References

1. D. Haidt, Eur. Phys. J. C **35**, 519 (2004)
2. C. Adloff et al., H1 Collab., Eur. Phys. J. C **21**, 33 (2001)
3. S. Chekanov et al., ZEUS Collab., Eur. Phys. J. C **21**, 443 (2001)
4. M. Glück, E. Reya, A. Vogt, Eur. Phys. J. C **5**, 461 (1998)
5. A.D. Martin, R.G. Roberts, W.J. Stirling, R.S. Thorne, Eur. Phys. J. C **23**, 73 (2002)
6. J. Pumplin et al., JHEP **7**, 12 (2002) [hep-ph/0201195]